

1-1-1964

Solid solubility of some rare-earth metals in gold

Paul Edward Rider
Iowa State University

Follow this and additional works at: <https://lib.dr.iastate.edu/rtd>

 Part of the [Chemistry Commons](#)

Recommended Citation

Rider, Paul Edward, "Solid solubility of some rare-earth metals in gold" (1964). *Retrospective Theses and Dissertations*. 18670.
<https://lib.dr.iastate.edu/rtd/18670>

This Thesis is brought to you for free and open access by the Iowa State University Capstones, Theses and Dissertations at Iowa State University Digital Repository. It has been accepted for inclusion in Retrospective Theses and Dissertations by an authorized administrator of Iowa State University Digital Repository. For more information, please contact digirep@iastate.edu.

SOLID SOLUBILITY OF SOME RARE-EARTH METALS
IN GOLD

by

Paul Edward Rider

A Thesis Submitted to the
Graduate Faculty in Partial Fulfillment of
The Requirements for the Degree of
MASTER OF SCIENCE

Major Subject: Physical Chemistry

Signatures have been redacted for privacy

Iowa State University
Of Science and Technology
Ames, Iowa

1964

TABLE OF CONTENTS

	Page
I. INTRODUCTION	1
II. THEORY OF SOLID SOLUTIONS	3
A. General Comments	3
B. The Size Factor	4
C. Electrochemical Factors	10
D. Valence Effects	13
III. EXPERIMENTAL	15
A. Materials	15
B. Preparation of Alloys	15
C. X-Ray Methods	17
D. Microscopic Examination	19
E. Thermal Analysis Methods	19
F. Treatment of the Data	20
IV. RESULTS	23
A. Solubilities	23
B. Eutectic Temperatures	34
V. INTERPRETATION OF RESULTS	35
A. Solubilities	35
B. Eutectic Temperatures	47
VI. CONCLUSION	51
VII. LITERATURE CITED	54
VIII. ACKNOWLEDGMENTS	56
IX. APPENDIX	57

I. INTRODUCTION

The behavior of solid solutions of one substance in another has been of great interest to chemists and metallurgists for some time. The existence of solid solutions was first recognized as far back as 1860 by Matthiessen and with the advent of the Gibbs phase rule at the turn of the century it became a generally recognized fact. Solid solutions are known to exist in both inorganic salts and metals. This study concerns the solid solubility behavior in binary alloy systems.

At the present state of development in solid solution theory certain basic criteria have been recognized which determine whether or not solid solutions will exist in binary metal systems. These criteria are closely aligned with the periodic nature of the elements but because of their simultaneous interplay it is difficult to describe them separately. The rare-earth metals offer a unique opportunity in testing these criteria. Hume-Rothery (1) was the first to recognize the factors which control solid solution formation in metal systems. There are three basic factors which are (a) the size factor (b) the electrochemical factor and (c) the relative valence factor. These are discussed in detail later but essentially if there are any large differences between two metals with respect to these factors the extent of their forming solid solutions will be seriously limited. In the rare-earth series, all of these factors are quite similar.

Because of their electronic structures, the rare-earth metals along with scandium, yttrium and lanthanum have metallic valences of 3 (except for europium and ytterbium which are divalent); electronegativities of around 1.20 e.V.; and atomic sizes which vary from 1.641A for scandium to 1.877A for lanthanum. Thus, from these considerations it is seen that the rare earths offer a valuable opportunity to contribute to the understanding of solubility and solid solutions.

Gold was chosen as the solvent in this study because of the results found by Wunderlin et al. (2) in the Ho-Au system. They found an abnormally high solid solubility for holmium in gold with regard to the Hume-Rothery criteria and it was felt that it would be of great interest to determine whether any other rare-earth in gold alloys might exhibit abnormal solubilities in gold.

II. THEORY OF SOLID SOLUTIONS

A. General Comments

Before discussing any detailed theory of solid solutions, a short mention of what is involved in the formation of a solid solution might be helpful.

The basic underlying factor which determines the nature of any natural process is the energy involved and the way it manifests itself in a system. Nature dictates the rules which the energy of a system obeys and any description of a natural process must consequently have its basis in the energy considerations of a system. When dealing with solid solutions the prime energy concern is the energy of the solvent. It is this energy which is changed upon addition of solute atoms to the solvent lattice. The degree to which this energy is changed depends upon the degree of difference between the characteristics of the solvent and solute atoms. If the degree of difference is small the amount of strain due to the introduction of a solute atom into the solvent lattice will not be too large and the solvent will tolerate a large amount of solute. The larger the degree of difference becomes, the more apt the system is to find a form which is energetically more favorable to nature (such as an intermediate phase or an intermetallic compound). If the degree of difference is too great, solid solution formation will not occur because

preference will be given to a form with lower energy than the solid solution, such as a compound.

Thus, it is easy to see why the solubility criteria of Hume-Rothery are so important. The size factor, electrochemical factor, and the relative valence factor are all closely related to the changes in energy involved in solid solution formation. Because all of these factors are manifestations of the energy of a system, they do not act independently of one another. Thus, in consideration of them it is essential to keep their simultaneous effects in mind.

B. The Size Factor

The effect of size difference on the energy of a solid solution is easy to visualize. For the most part, metals exist in close-packed structures having high packing efficiencies. By introducing an atom of differing size into the lattice of the solvent, the atoms of the solvent are forced to accept new positions resulting in a higher energy configuration than that of pure solvent. This is the source of a strain energy in the system.

The shifting of the solvent atom positions due to size differences is also the crucial point of the method used to determine solubilities in this study. This change is reflected in a change in the lattice constant of the solvent. Vegard (3) first recognized this behavior in 1921 while investigating

solid solutions of inorganic salts such as KCl and KBr. Vegard noted that the lattice constants of solid solutions were linear combinations of the lattice constants of the two pure components; i.e.

$$a_{\text{alloy}} = f_1 a_1 + (1 - f_1) a_2$$

where,

$$\begin{aligned} a_{\text{alloy}} &= \text{lattice constant of the alloy} \\ a_1 &= \text{lattice constant of component 1} \\ a_2 &= \text{lattice constant of component 2} \\ f_1 &= \text{fraction of component 1 present} \end{aligned}$$

This expression is often referred to as "Vegard's law". In 1928 (1) this principle was said to apply to metallic solid solutions but deviations from it have been found to exist in practically all binary alloy systems by Hume-Rothery and others (1). Both Eshelby (4) and Friedel (5) have attributed deviations from Vegard's law to the product of the difference in the size and the difference in the compressibility of the atoms involved. Accordingly, only solid solutions having atoms with either identical sizes or compressibilities would be expected to obey Vegard's law. Oschneidner and Vineyard (6) have compared several methods of explaining deviations from Vegard's law and have proposed one based on second-order elastic theory which allows fairly good prediction of Vegard's law deviations compared to other methods.

The changing of the lattice constant of a solid solution upon addition of more solute leads, quite naturally, to the

question of what is that actual nature of a solid solution. As a first approximation one would assume that the solute would be randomly distributed throughout the solvent. However, Averbach (7) mentions that according to diffuse x-ray analysis results, there are very few random solid solutions and instead there is a tendency toward ordering or clustering. In a solid solution there are areas of severe local distortion (around solute atoms) surrounded by areas of very little distortion. The lattice constant for a solid solution, is thus, an "average" constant and does not actually represent the distance between any particular atoms. Warren, Averbach, and Roberts (8) have shown this through diffuse x-ray analysis. Their results show that the diffraction pattern of a solid solution contains lines produced by an "average lattice" and that the atoms are offset from the points of this lattice by a slight amount. It is this average lattice which shows a uniform expansion upon addition of solute and this is reflected in the linear change of the lattice constant.

In using the size factor for predicting solid solution formation, there is difficulty in defining what is meant by an atom's size. The metal atom is often treated as a hard sphere and for a good many cases this does not lead to appreciable error. But because the apparent nature of an atom in which it is pictured as a central nucleus surrounded by a diffuse electron cloud, the term "size" takes on an aspect of ambiguity.

Hume-Rothery, Mabbot, and Chennel-Evans (1) have observed that if the sizes of two atoms differ by more than 14 percent to 15 percent solid solution formation is restricted between those atoms. To use this value, or "size factor", the difficulty lies in the fact that the atom has a variable size which is a function of its environment. Several methods have been devised for assigning values to the atomic radii of metals. Goldschmidt (9) used the basic crystal structure of metals to determine atomic size. Since a great many metals have h.c.p. or f.c.c. structures, he based his scheme on these structures with coordination number 12. He took the radius to be one-half the distance between two successive atoms in either structure. In order to predict the size of an atom having a normal CN12 in another structure, he reduced the CN12 radius by a certain amount (i.e. 4 percent for b.c.c. and 12 percent for the diamond structure). For alloys he assumed Vegard's law to be valid and extrapolated the lattice constant for the solid solution to 100 percent solute. This gave an "apparent atomic diameter (or radius)" for the solute atom as if it crystallized in the same structure as the solvent. Radii calculated in this manner, however, only applied to the alloys being investigated. Hume-Rothery and Raynor (1) took the atomic diameter to be the distance of closest approach of the atoms in the normal structure of the metal. They recognized the difficulties connected with this choice such as the incomplete ionization of some metals in various alloys (e.g.

indium, tin, and lead), the structure of some metals which have abnormally short bond distance of low coordination number (e.g. gallium) and also the existence of different allotropic modifications for many metals. To account for the variable size of atoms they pictured atoms as being "open" or "filled", according to the volume of the total atom occupied by the valence electrons. Open metals have small ion-core radii compared to the total atomic radii and filled metals have ion-core radii and atomic radii nearly the same. The alkali metals have examples of open metals and the noble metals of filled metals. Axon and Hume-Rothery (10) developed this idea in terms of a quantity, V_e , the volume per valence electron in a metal. Open metals have a large V_e while filled metals have a small V_e . As a result, open metals have a more compressible structure than filled metals. This means that solid solutions of open metals in filled metals will result in negative deviations from Vegard's law and the opposite will be true for solutions of filled metals in open metals.

Warren, Averbach, and Roberts (8) used diffuse x-ray analysis for still another way of determining atomic size. In this method, they were able to measure the distance between nearest neighbor atoms in solid solutions from the amount of diffuse scattering of x-rays from solid solution alloys. Their results showed that, generally, the sizes of both solute

and solvent atoms were functions of composition. There appeared to be a tendency in some instances for both atoms to approach the hypothetical size of an atom derived from the lattice constant of the average lattice. However, they found exceptions to this behavior, notably gold in nickel and platinum in copper.

Chessin, Arajs, and Miller (11) have recently developed a new scheme for estimating atomic radii. Their method involves dividing the unit cell volume by the number of atoms per unit cell to get the volume per atom. From this they calculate the atomic radius. In this approach the atom is pictured as having two volume elements. One is the volume of the ion core which is incompressible and the other is the volume of the valence electron shell which is compressible. The ion cores are relatively close-packed with the valence electrons being smeared out into the empty areas of the lattice. To determine the size of a solute atom in a crystal structure differing from its own parent structure they (1) calculated the compressible and incompressible volumes of the atom in the parent structure; (2) assumed the incompressible volume to remain constant; and (3) used packing efficiencies to determine the volume available for the valence electrons in the new structure. By using a linear relationship analogous to Vegard's law they were able to calculate lattice constants for germanium in iron solid solutions in

almost exact agreement with experimental values.

C. Electrochemical Factors

The electrochemical factors are not as readily understood as the size considerations. Because of the complex nature of the electronic structure of metals and the ways in which the electrons in a metal behave, it is difficult to give solid quantitative theory for the role of electronic considerations in solid solution behavior. One of the electrochemical factors to be considered is the electronegativities of the atoms. Basically, this is a measure of the tendency of an atom to attract electrons to itself. If the members of a solid solution have widely differing electronegativities, one member will tend to accumulate electrons at the expense of the other with the result being ionic bond formation (and consequently compound formation). Such behavior limits solid solution formation. From a thermodynamic standpoint, large electronegativity differences favor chemical interaction because they lead to negative contributions to the excess entropy, enthalpy, and free energy of a system (12).

Another effect which is actually more closely aligned with the valences of the components but still related to their electronegativities involves the change in energy in the electronic distribution caused by a perturbation potential associated with the introduction of a solute atom into the solvent lattice. If the ionization energy of the solute is

different from that of the solvent there will be a charge build-up of electrons around the solute or solvent atoms (depending on which has the higher ionization energy). Slater and Koster (13) discuss this sort of behavior in terms of a perturbing potential, V_p , which modifies the energy and motion of the valence electrons. There is a critical value below which there is not a very large effect on the electron distribution and above which "bound" electron energy states become separated from the conduction bands of the valence electrons. These bound states are closely aligned with bond formation. Friedel (14) described V_p as causing rigid displacement of the conduction bands. The Fermi energy remains at a constant absolute energy and the top or bottom of the band moves toward it under the influence of V_p . The bound states separate from either the top or bottom of the conduction bands. That this is actually a valence effect is evident from Friedel's expression for V_p which involves the valence difference of the two solution components. Jones (15) used the rigid band model to explain the limiting effects of valency differences in copper, silver, and gold. The Fermi energy in these metals, which represents the free energy of the valence electrons in a metal, is inversely proportional to the density of occupied states in the valence shell. The density of states in the rigid band model will depend on the average number of valence electrons per atom which metallur-

gists refer to as the "e/a" (electron per atom) ratio. Thus as e/a increases, when a polyvalent solute is added to copper, silver or gold, the density of states decreases and correspondingly the Fermi energy increases. At a certain e/a ratio the electronic distribution will come in contact with a forbidden energy gap of the Brillouin zone and the density of states curve will begin to decrease very rapidly, resulting in a rapid increase in energy. Any new phase which has a still lower free energy is then available to the system and will be favored over a solid solution. Thus, the e/a ratio limits the solubility range.

With respect to quantitative limits on the electronegativity difference, Darken and Gurry (16) place a difference of ± 0.4 e.v. as the point where two solution components will display negligible solid solubility. There are different methods of determining electronegativity so that comparisons between atoms must be consistent with the method used. Pauling (17) developed a scale based on the heats of formation of bonds between two unlike atoms. Gordy and Thomas (18) developed an empirical relationship between the number of valence electrons and the single-bond covalent radius of an atom to calculate its electronegativity. Both scales are quite similar except for copper, silver and gold.

D. Valence Effects

The effects of valence have been discussed previously in terms of the e/a ratio and its effect on the energy of an alloy.

Another principle which should be mentioned is the relative valence effect described by Hume-Rothery (1). According to this principle, the tendency for two metals to form solid solutions is not necessarily reciprocal. This is illustrated in the situation in which lower valent solvents tend to dissolve higher valent solutes more readily than in the reverse case. This situation holds true most always for univalent solvents and polyvalent solutes, but the case for higher valent solvents is more confusing and exceptions are known (such as the In-Mg system). Kleppa (12) discusses the thermodynamics behind this principle and indicates that there exists an asymmetry in the thermodynamic functions for solutions of component one in component two in comparison to the reverse situation. He discusses it in terms of the limiting curvature of the enthalpy of mixing which is dependent upon the valence difference of the two solution components. Positive curvatures result for the case of polyvalent solutes and univalent solvents, meaning that the solute atoms tend to repel each other, which favors solid solution formation. For the reverse case, negative curvatures result with an attraction occurring

between solute atoms, which does not favor solid solution formation. These results give some basis to the Hume-Rothery relative valence effect.

III. EXPERIMENTAL

A. Materials

The gold used in this investigation was obtained from the Williams Gold Refining Company of Buffalo, New York. It has a purity of 99.99 percent with respect to non-gaseous impurities. No gas analysis was run on the gold because of its relative inertness toward the gases in the air.

The rare-earth metals were obtained from the Ames Laboratory of Iowa State University, Ames, Iowa. The metals used were scandium, yttrium, lanthanum, cerium, neodymium, samarium, gadolinium, terbium, dysprosium, holmium, erbium, thulium, ytterbium, and lutetium. The impurity analysis of these metals are given in Table I.

B. Preparation of Alloys

Two or three gram alloy samples were prepared by arc melting gold and the particular rare earth, which had been weighed out to ± 0.1 mg. in the desired composition.

After the metals were melted and held in the liquid state for a few seconds, they were allowed to freeze and were turned over and re-melted. This process was repeated three or four times to insure homogeneous mixing of the metals. The samples were re-weighed to determine any weight losses from melting. With the exception of some of the Er-Au alloys, all alloys

Table 1. Analyses of the rare-earth metals (ppm)(trace refers to a slight indication of the presence of an element)

Rare-earth	O ₂	H ₂	N ₂	Fe	Si	Ta	Ca	Sm	Ba	Tb	Y	Hg	Cr	Dy	Yb	Ho	Tm	Gd	Er	Tm	La	Ce	
Sc	-	100	-	38	160	250	20	-	-	-	-	25	35	-	-	-	-	-	-	-	-	-	-
Y	380	175	130	100	-	-	-	-	-	-	-	-	-	-	-	-	-	-	-	-	-	-	-
La	350	20	100	10	50	200	5	-	-	-	-	-	-	-	-	-	-	-	-	300	200	-	300
Ce	183	11	5	25	15	1000	25	-	-	-	-	-	-	-	-	-	-	-	-	200	200	200	-
Pr	387	4	44	100	50	500	100	100	-	-	100	-	-	-	-	-	-	-	-	1000	-	-	-
Sa	7	117	10	20	tr	-	100	-	10	-	tr	30	10	-	tr	-	-	100	-	-	200	tr	-
Gd	1730	11	245	60	25	2500	5	200	10	100	20	-	-	-	-	-	-	-	-	-	-	-	-
Tb	-	-	7	-	tr	-	tr	-	-	-	-	-	-	200	-	-	-	100	-	-	-	-	-
Dy	446	-	-	150	50	400	300	-	-	500	50	50	-	-	-	100	-	100	50	-	-	-	-
Er	162	17	10	800	50	500	200	-	-	-	50	500	200	200	200	50	100	-	-	-	-	-	-
Tm	-	-	41	50	100	2000	200	tr	-	tr	-	-	-	-	tr	-	-	-	-	-	-	-	-
Yb	-	-	-	200	100	-	100	-	-	-	100	-	-	-	-	-	10	-	50	-	-	-	-
Lu	1500	12	165	25	15	200	10	-	-	-	-	-	-	-	-	-	-	-	-	-	-	-	-

had weight losses of 0.5 percent or less so that the compositions were not seriously altered. The weight losses in the first five Er-Au alloys, which were the first alloys prepared in this study, ranged from 2.0 percent to 5.0 percent but two additional alloys prepared later on had weight losses of less than 0.5 percent. The results of these last alloys fit in well with those of the first alloys, indicating that the weight losses were not due to one component alone but were rather due to loss of both gold and erbium.

After arc melting, the alloys were wrapped in tantalum foil, then placed in quartz tubing, and sealed off under a partial atmosphere of argon. They were placed in a resistance furnace for approximately 200 hours at 780°C. This particular temperature was chosen because it corresponded to the eutectic temperature found by Wunderlin et al. (2) for the Ho-Au system (this temperature was later found to be in error). A second set of Tb-Au alloys were prepared and these were annealed at 809°C., the eutectic temperature of gold-rich Tb-Au alloys. After the prescribed annealing period the alloys were removed from the furnace and quenched in cold water.

C. X-Ray Methods

The x-ray parametric method was used in determining the solubility of the rare-earth metals in gold. In this technique the lattice parameters of the alloys are plotted as a function of composition. In a single phase region, in general,

the lattice parameters change as the composition changes; that is, the slope is non-zero. In a two phase region the lattice parameters remain constant; that is, the slope is zero. The composition corresponding to the intersection of these two lines represents the solubility limit at the temperature from which the alloys were quenched.

In order to determine the lattice parameters of the alloys, filings from the heat-treated specimens were placed in small tantalum tubes which in turn were then sealed under an inert helium atmosphere. The tantalum tubes were then sealed in quartz tubing under a partial argon atmosphere and were placed in the resistance furnace at various annealing temperatures. The time of annealing ranged from one-half hour to three hours (the length of time was inversely proportional to the annealing temperature). The samples were then quenched in cold water and placed in 0.3 mm. diameter glass capillaries for x-ray photographs.

X-ray patterns of the samples were taken by using a 114.6 mm. Debye-Scherrer camera and copper K α radiation. The optimum exposure time for the samples was found to be approximately two hours.

The spacings of the (331), (420), (422), and (333) sets of back reflection doublets were measured on each pattern. From these data, the lattice constants for the solid solutions of the rare-earth metals in gold were calculated by using the

⊕tan⊕ extrapolation procedure. Lattice constant versus composition curves were constructed for each system.

D. Microscopic Examination

To confirm that the lattice constant versus composition curves were valid, the samples in the Gd-, Er-, and Lu-Au systems which lay on either side of the solvus line on the gold-rich end of the phase diagrams were examined metallographically.

The alloys were mounted in bakelite, polished, and etched with aqua regia. In all systems the alloy which was expected to lie in the one phase region according to the established solvus line was found to be one phase and the alloy which was expected to lie in the two phase region was found to contain two phases. This confirmed the solvus curves determined by the x-ray parametric method.

E. Thermal Analysis Methods

The eutectic temperatures for the rare-earth-gold systems were determined using thermal analysis. Twenty-gram alloys with 12 atomic percent rare earth in gold were prepared by using the methods in part B. After 200 hours of heat treatment the alloys were loaded into cylindrical tantalum crucibles, 0.95 cm. diameter x 3.8 cm. length, with 0.32 cm. diameter x 0.64 cm. length thermocouple wells. The crucibles

were sealed under a helium atmosphere.

Thermal analyses were run under a partial helium atmosphere using a tantalum tube resistance heater and vacuum furnace. The eutectic temperatures were taken to be the first thermal arrests on the heating curves of each sample. These arrests were also confirmed on cooling curves. The eutectic temperature was taken as the mean value of two or more heating and cooling cycles.

F. Treatment of the Data

Any set of data are subject to both random and systematic errors. Random errors result from the taking of data and are chance errors, subject to the bias of the investigator. Systematic errors occur because of the inherent imperfections and weaknesses of the methods and equipment used in obtaining the data.

In order to determine accurate lattice parameters, it was necessary to minimize the systematic errors involved in the Debye-Scherrer technique. The four most important systematic errors in this method are: the incorrect camera radius, film shrinkage, the eccentricity of the sample, and the absorption of x-rays by the sample. A $\phi \tan \phi$ extrapolation procedure was used in this investigation to minimize these sources of error. In this procedure, the error is expressed as a function of ϕ (the complement of the Bragg angle θ) in the form of $\tan \phi$.

This error function is extrapolated to

$$\phi = \tan\phi = 0$$

at which point the error theoretically becomes zero. A more detailed discussion of this procedure is given by Cullity (19).

Another cause of error was in the weight losses incurred by the alloys during melting. This error in composition was regarded as negligible because, for example, in the 1.0 percent and 4.0 atomic percent samples in the Lu-Au system the weight losses were such that the compositions of these alloys would have been shifted to 0.8 atomic percent Lu and 3.2 atomic percent Lu respectively, if all of the weight loss were due to lutetium. Yet in the 2.0 atomic percent Lu alloy the weight loss was greater than the original amount of lutetium present and still the lattice constant for the 2.0 atomic percent alloy lay on the line drawn between the lattice constants for the 1.0 atomic percent and 4.0 atomic percent alloys. This indicated that the weight losses were due to loss of both rare earth and gold in ratios comparable to the originally intended compositions. If all of the weight loss were due to gold, the original compositions would not have been changed significantly. It is possible that the weight losses were not in ratios comparable to the originally intended compositions but since the gold was melted "over" the rare earth the weight

loss was probably largely attributable to the initial striking of the arc which hit the gold first and consequently the compositions were not seriously altered.

IV. RESULTS

A. Solubilities

To determine the solubilities of the light rare-earth metals, lanthanum, and yttrium in gold, gold-rich alloys containing 3.0 atomic percent Y, 4.2 atomic percent La, 5.9 atomic percent Ce, 5.2 atomic percent Nd, and 4.0 atomic percent Sm were prepared. It was felt that if these alloys had lattice constants only slightly different from that of pure gold then this would indicate a rather small solubility for these metals in gold. Table 10 in the Appendix shows the results and as can be seen, there are only slight increases in the lattice parameters for these alloys compared to pure gold, except for yttrium in gold. This suggests that these metals are slightly soluble in gold. The annealing temperature for all of these alloys was 765°C . For the La-Au alloy a second specimen was re-examined at 798°C . (the eutectic temperature for gold-rich La-Au alloys). The value of the lattice constant at this temperature was approximately the same as that at 765°C ., indicating that there is not a sharp increase in solubility near the eutectic temperature. The relatively large change in the lattice constant of gold caused by the yttrium addition indicates there might be a significant solubility for yttrium in gold.

Estimates of the solid solubility limits of these metals in gold were made from the data of the other rare earth-gold systems and are shown in Table 2. The details of the procedure used to make these estimates are given in the section on Interpretation of Results, A. Solubilities.

Table 2. Solubility of light rare-earths, Y, and La in gold

Alloy system	Estimated solid solubility limit
Y-Au	2.0 a/o
La-Au	0.1-0.2 a/o
Ce-Au	0.2-0.3 a/o
Nd-Au	0.2-0.3 a/o
Sm-Au	0.3 a/o

The compositions for the alloys used in determination of the solubilities of the heavy rare-earth metals and scandium in gold are given in Table 3.

The results for the solubilities are shown in Figures 1 through 7. The lattice constant versus composition curves are given in the upper portion of the figures. The various annealing temperatures are listed alongside the horizontal lines. The terminal solid solubilities of the various rare earths in gold are given in the lower part of the figures. The Gd-Au data are shown in Figure 1, the Tb-Au in Figure 2, the Dy-Au in Figure 3, the Er-Au in Figure 4, the Tm-Au in Figure 5, the Lu-Au in Figure 6, and the Sc-Au in Figure 7.

Table 3. The compositions of alloys used for solubility determinations (heavy rare earths)

Alloy system	Composition (at% R.E.)
Gd-Au	0.3, 0.5, 1.0, 1.5, 2.0, 3.0, 4.0
Tb-Au	0.5, 1.0, 2.0, 3.0
Dy-Au	0.5, 1.0, 2.0, 3.0, 4.0, 5.0
Er-Au	0.6, 1.2, 2.3, 3.5, 4.7, 6.0, 8.0
Tm-Au	2.0, 4.0, 6.0, 8.0
Lu-Au	2.0, 4.0, 6.0, 8.0
Sc-Au	3.0, 6.0, 9.0, 12.0

Terbium in gold alloys were prepared twice because the results from the first alloys were not consistent with those of the other rare earth-gold alloys. Apparently, during annealing, the quartz tubing cracked and the inert atmosphere was replaced by air. The samples absorbed either nitrogen or oxygen or both. Hansen (20) states that pure gold does not dissolve either of these gases but apparently the terbium-gold alloys did. The largest weight gain (0.6 percent) due to absorption of air occurred in the alloy with the largest terbium content. The lattice parameters of these alloys are shown in the upper portion of Figure 2. Comparing these results with those of the second set of alloys (shown in the

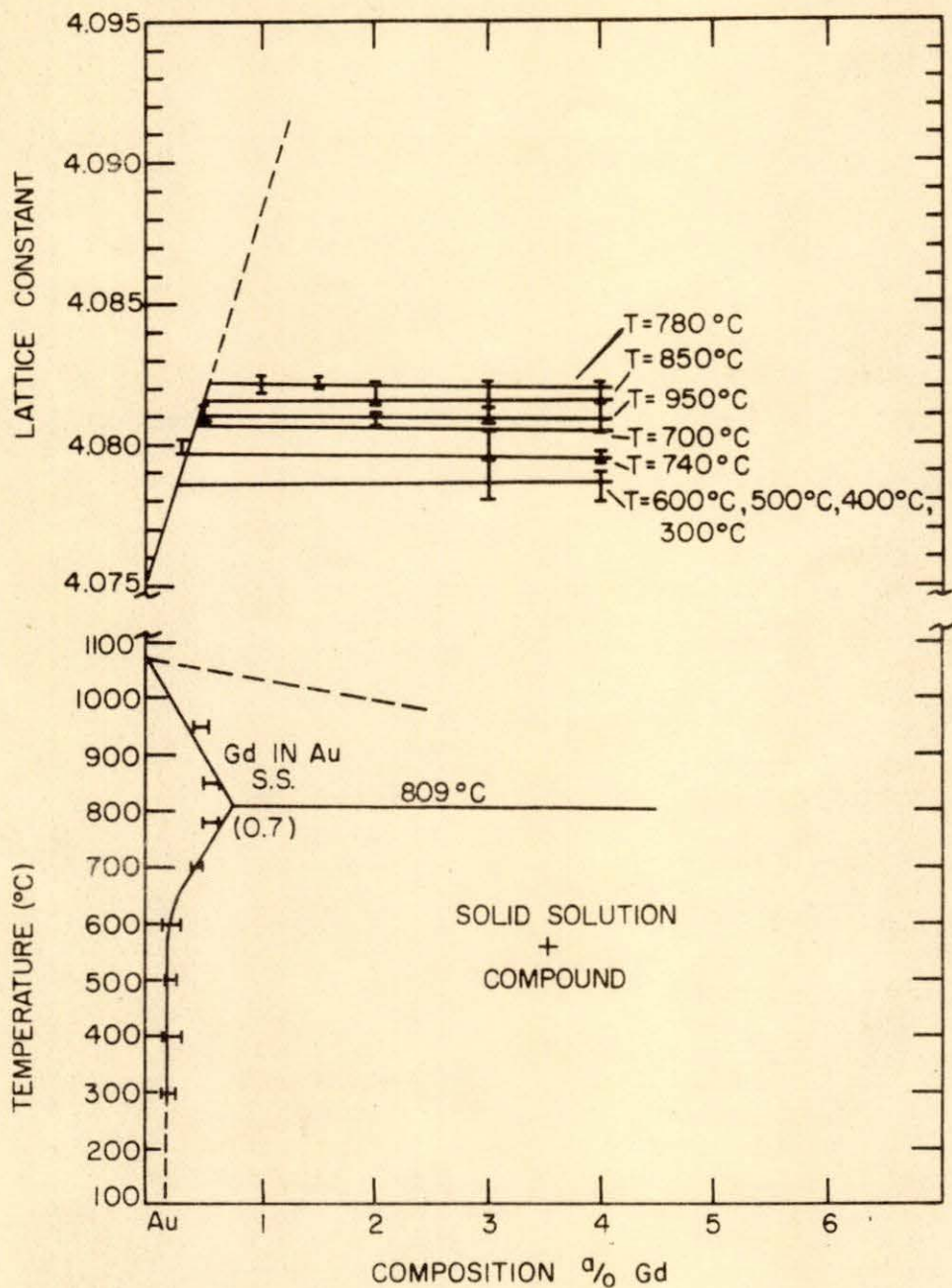


Figure 1. The Gd-Au system. The upper portion shows the lattice constant as a function of composition, the lower portion the solid solubility limits as a function of temperature.

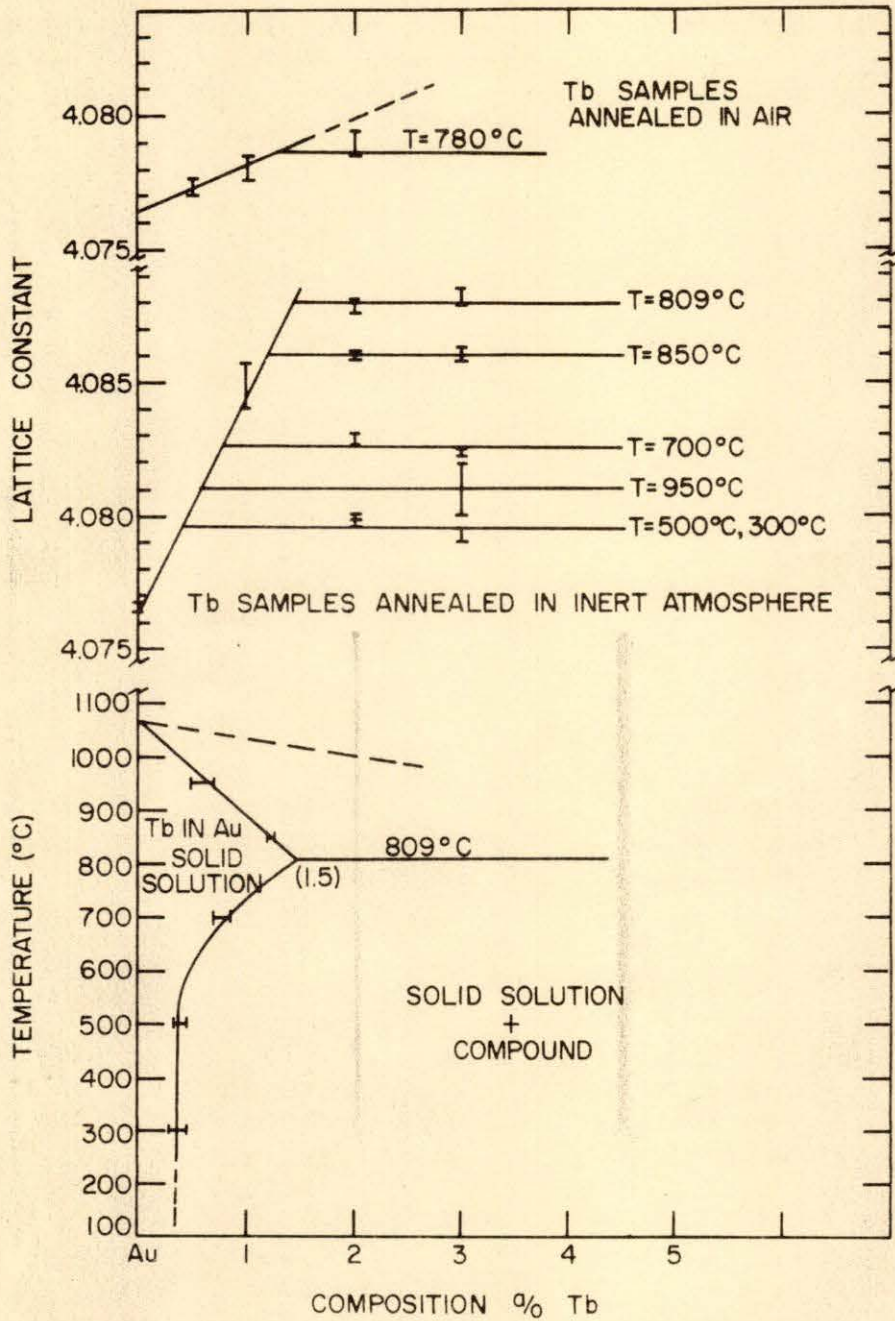


Figure 2. The Tb-Au system. The upper portion shows the lattice constant as a function of composition, the lower portion the solid solubility limits as a function of temperature.

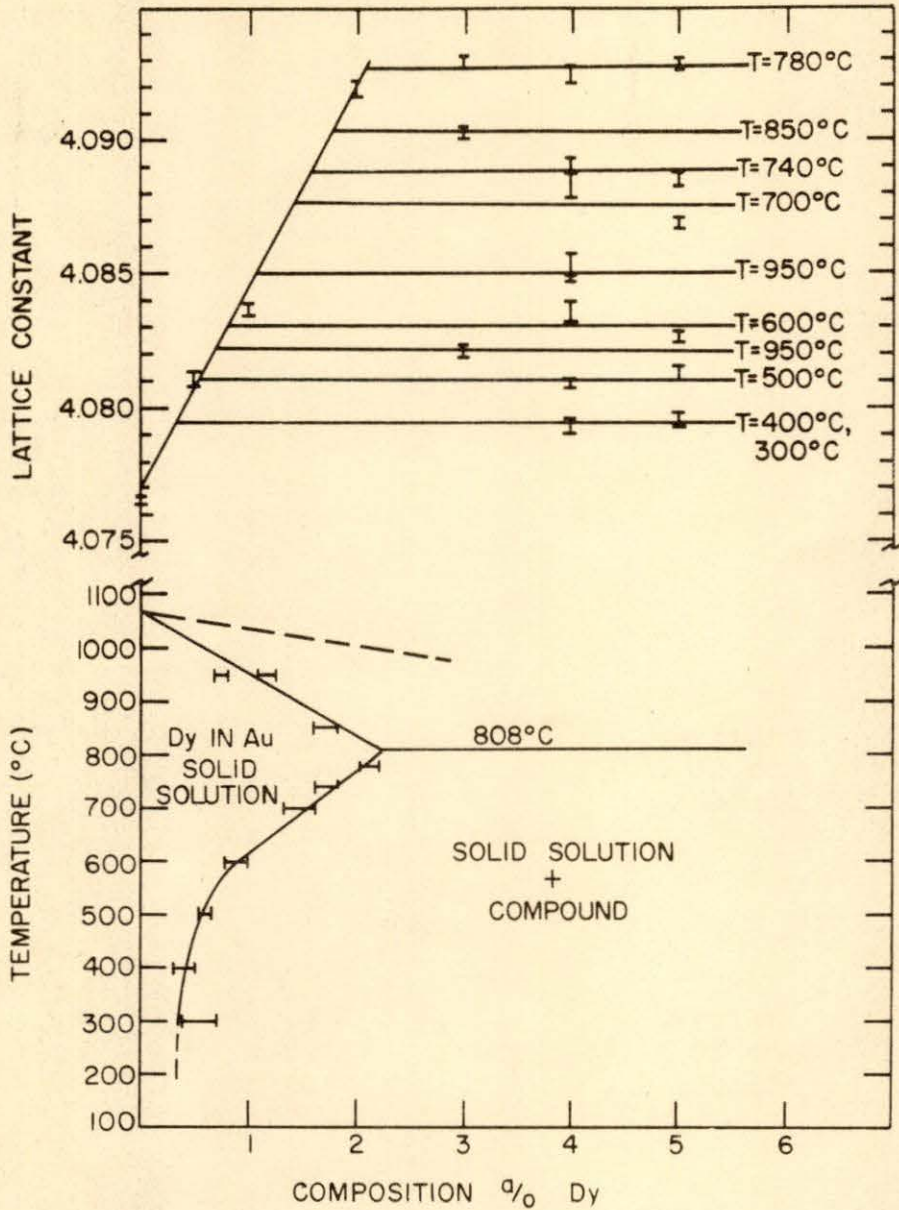


Figure 3. The Dy-Au system. The upper portion shows the lattice constant as a function of composition, the lower portion the solid solubility limits as a function of temperature.

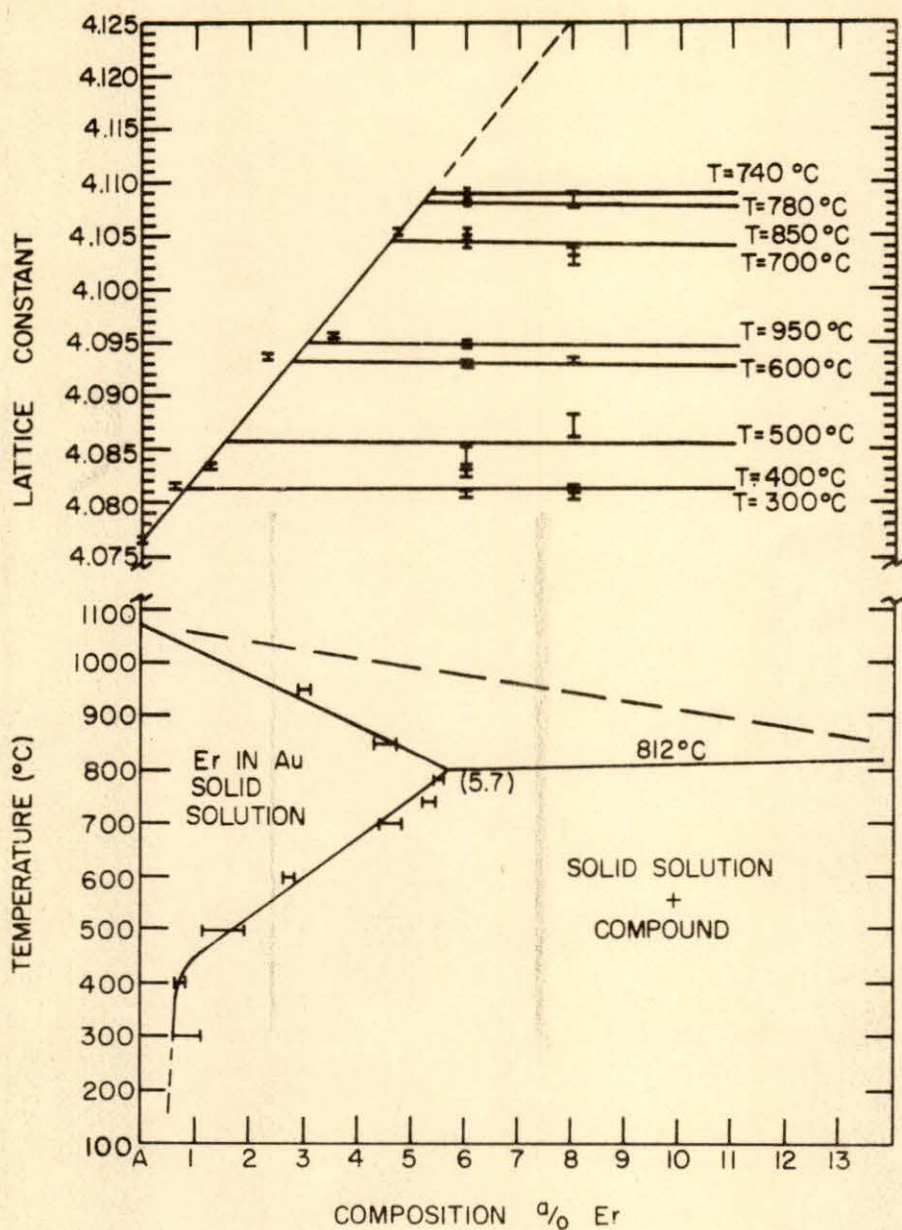


Figure 4. The Er-Au system. The upper portion shows the lattice constant as a function of composition, the lower portion the solid solubility limits as a function of temperature.

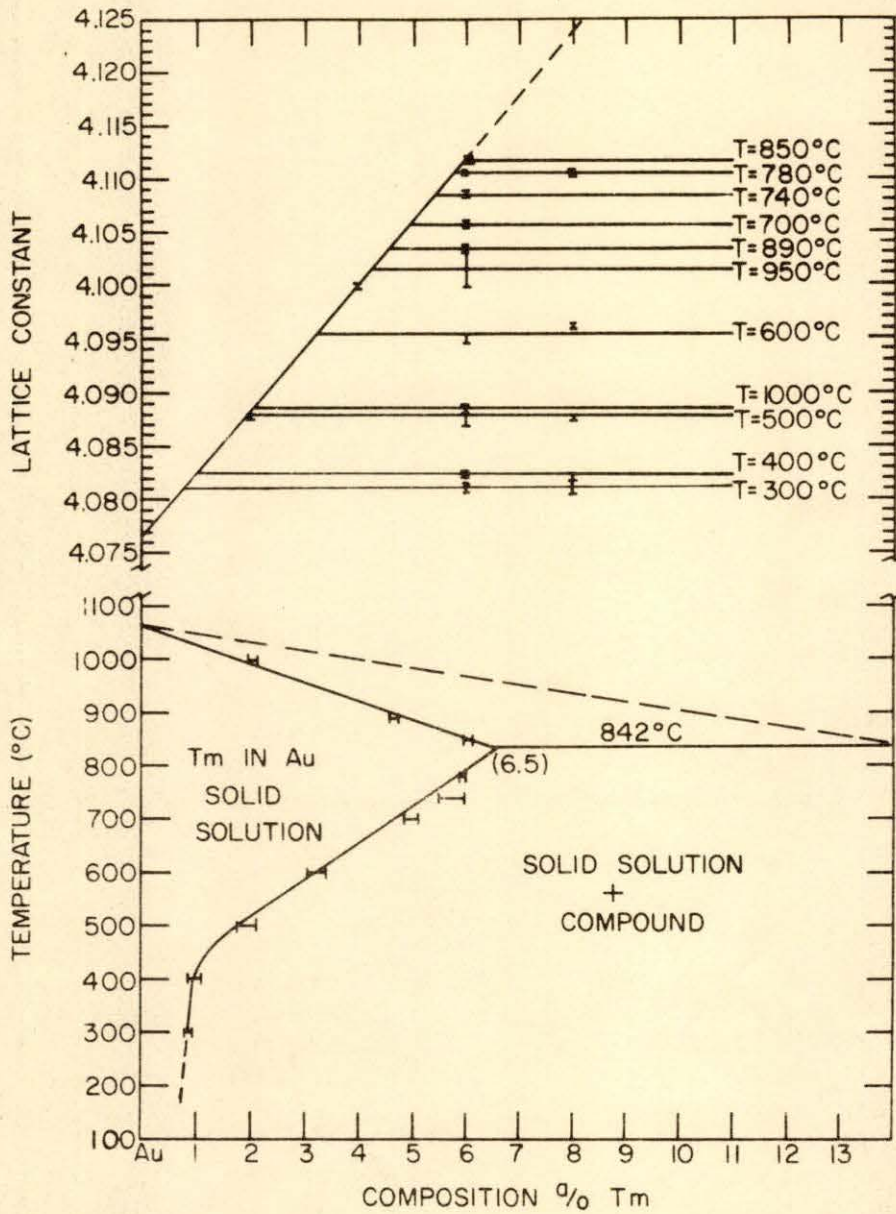


Figure 5. The Tm-Au system. The upper portions shows the lattice constant as a function of composition, the lower portion the solid solubility limits as a function of temperature.

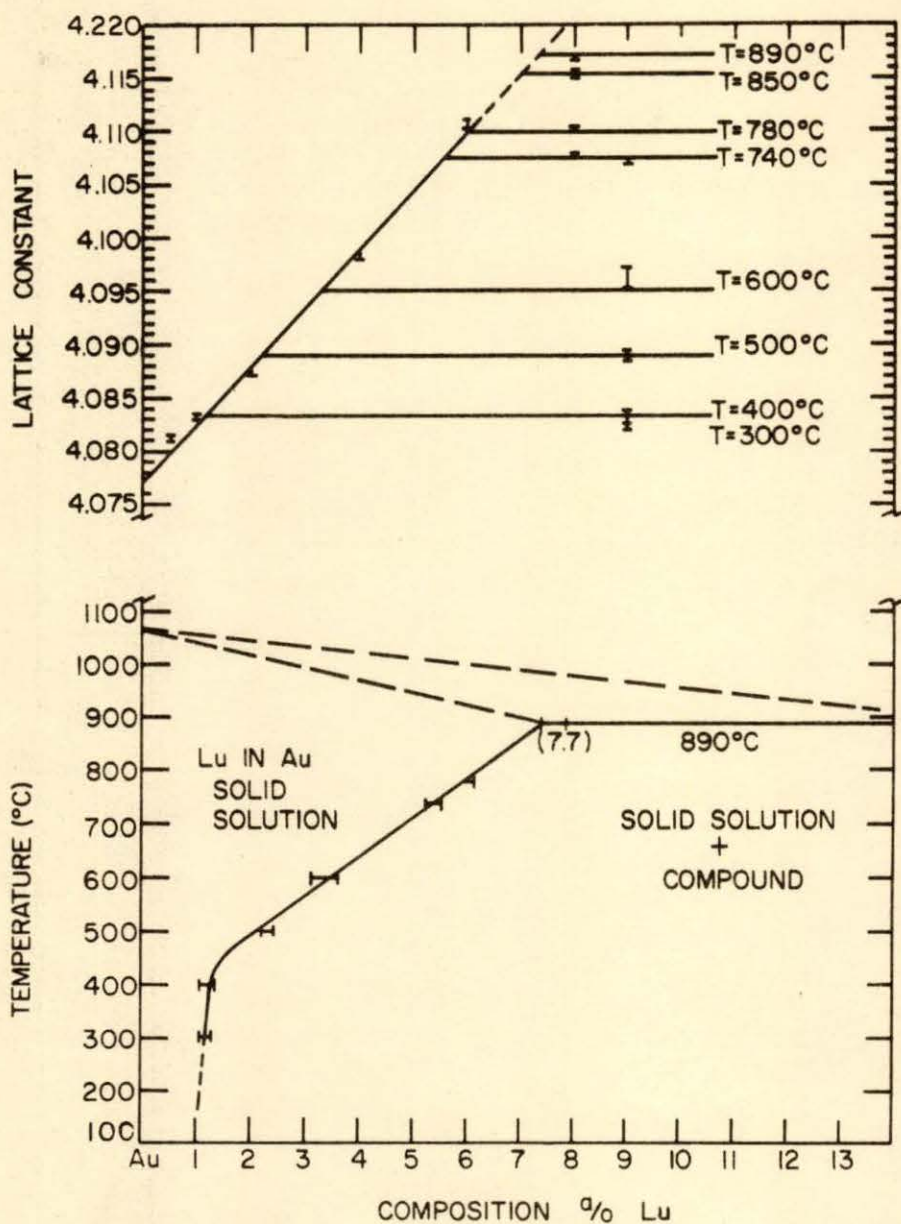


Figure 6. The Lu-Au system. The upper portion shows the lattice constant as a function of composition, the lower portion the solid solubility limit as a function of temperature.

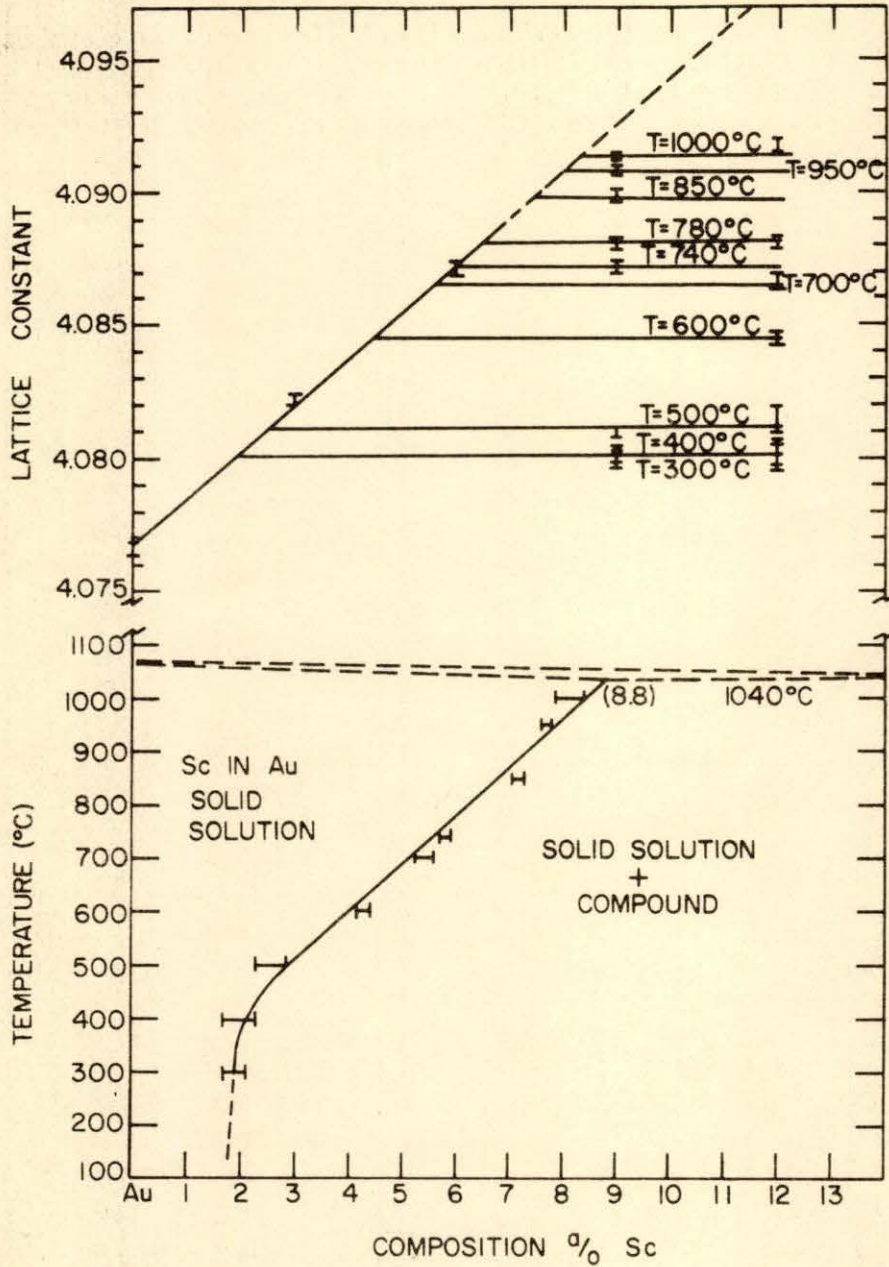


Figure 7. The Sc-Au system. The upper portion shows the lattice constant as a function of composition, the lower portion the solid solubility limits as a function of temperature.

middle portion of Figure 2) it is seen that the lattice constant versus composition curve is flattened out by the presence of oxygen or nitrogen in the samples. But it is interesting to note that the solubilities at 780°C . for the contaminated and uncontaminated alloys are the same.

In the Dy-Au system, both the 3.0 and 4.0 atomic percent alloys were annealed at 950°C (Figure 3). The lattice parameters in these two alloys differed by approximately 0.003 Å indicating a solubility between 0.75 and 1.20 atomic percent Dy. Since no preference could be given to either alloy both points are included in the figure.

The scatter of the data points about the line for the Er-Au system is due to the large weight losses incurred in melting the first samples. The line as drawn is in reasonable agreement with the other rare earth-gold systems.

No data points were obtained above the eutectic temperatures in the scandium and lutetium in gold systems. This was due to the closeness of the eutectic temperature in the Sc-Au systems to the melting point of gold and difficulties encountered in attempting to get well defined x-ray patterns in the Lu-Au system.

The experimental data for all these systems are given in Table 11 in the Appendix.

B. Eutectic Temperatures

The eutectic temperatures determined by thermal analysis techniques in this study and some literature values for the rare earth-gold systems are listed in Table 4.

Table 4. Eutectic temperatures for rare earth-gold systems

Rare earth (Rare-earth-gold systems)	Eutectic temperature ($^{\circ}\text{C}.$)
La ^a	798
Ce ^a	808
Pr ^a	809
Gd	809
Tb	809
Dy	808-809
Ho	808-809
Er	812
Tm	842
Lu	890
Sc	1042
Y	809

^aValue from Gschneidner (21).

As is seen, the eutectic temperatures of the lanthanide-gold systems remain fairly constant as one proceeds along the series of elements until erbium is reached. At erbium the eutectic temperature begins to increase and rises to a value of $890^{\circ}\text{C}.$ for lutetium in gold. Scandium which is even smaller than lutetium has a much higher eutectic temperature ($1042^{\circ}\text{C}.$). Yttrium which is about the same size as gadolinium has an eutectic temperature which is the same as the majority of the lanthanides which have atomic numbers less than that of erbium (at. no. 68).

V. INTERPRETATION OF RESULTS

A. Solubilities

In view of the previous discussion, the solubilities observed in the heavy rare earth-gold systems would not be expected because as is shown in Table 5, two of the three Hume-Rothery criteria are not favorable and the third, the relative valence factor, may or may not be favorable. The size factors in all cases are in excess of the 15 percent value by a rather large degree. The smallest rare earth, lutetium, differs by about 20 percent in size and yet shows a solubility of almost 8.0 atomic percent in gold. Even dysprosium which is 23 percent larger than gold shows a solubility of over 2.0 atomic percent. The size factor for scandium is within the favorable range for gold (13.8 percent) and it shows the largest solubility (8.8 atomic percent). However, the size factor for lutetium is one and one-half times as large as that for scandium yet the solubilities are only one atomic percent apart. Apparently, in accord with the discussion of the theory, the sizes of the heavy rare-earth atoms and possibly that of gold change in the alloys of the two so that they are more nearly the same size. Changes in electronic structure or possibly the compressibility of the atoms might account for these changes.

The electronegativities of gold and the rare-earth atoms differ by more than the 0.4 e.v. limit proposed by Darken and

Table 5. Data for predicting solubilities (rare-earth-gold systems)

Element	Radius r(A)	Electroneg. χ^a	Valence	Size diff. ($r_{RE}/r_{Au} - 1$)100	Electroneg. diff. ^b
Y	1.801	1.20	3	24.9	0.70
La	1.877	1.17	3	30.2	0.73
Ce	1.825	1.21	3	26.6	0.69
Nd	1.821	1.19	3	26.3	0.71
Sm	1.802	1.18	3	25.0	0.72
Gd	1.802	1.20	3	25.0	0.70
Tb	1.782	1.21	3	23.6	0.69
Dy	1.773	1.21	3	23.0	0.69
Er	1.757	1.22	3	21.8	0.68
Tm	1.746	1.22	3	21.1	0.68
Lu	1.734	1.22	3	20.3	0.68
Sc	1.641	1.27 ^c	3	13.8	0.63
Au	1.442	1.90 ^c 2.30 ^d	1	-	-

^aValue based on Gordy scale (18).

^bCalculated using value (c) for gold.

^cValue taken from Wabet *et al.* (22).

^dValue from Gordy and Thomas (18).

Curry (16). The value of 1.9 for gold was taken from a paper by Waber *et al.* (22) rather than the value of 2.3 given by Gordy and Thomas (18) as a "selected value" for gold, because Waber *et al.* (22) have shown that the 2.3 value is too high to explain the metallurgical nature of gold with respect to the formation of solid solutions. Even this lower value is almost 0.7 units larger than the values for the rare earths, and would appear to hinder any solid solution formation.

The valence difference of two between gold and the rare earths would also seem to limit the amount of solid solution formation between them in comparison with the solubility of a divalent metal in gold.

Some interesting results were obtained by extrapolating the lattice constant versus composition line to 100 percent rare earth to obtain the apparent atomic radii of the rare earths. Table 6 gives the apparent atomic radii calculated by this method and the corresponding size differences.

Table 6. Apparent atomic radii and size factors (rare earth atoms in gold)

Rare earth	Radius a.s.r.	$(r_{R.E.} - r_{Au}/r_{Au})100$	Solid sol. limit (a/o)
Sc	1.507	4.5	8.8
Lu	1.629	13.0	7.7
Tm	1.644	14.0	6.5
Er	1.656	14.8	5.7
Dy	1.689	17.1	2.3
Tb	1.712	18.7	1.5
Gd	1.772	22.8	0.7

As can be seen, there is a significant drop in the solubility between erbium and dysprosium as the size factor exceeds 15 percent. If the rare earths have these sizes in solution with gold, then the Hume-Rothery (1) criterion of 15 percent size difference seems to be satisfied. Again, it is significant that in the case of scandium and lutetium the size factor for lutetium is now three times as large but the solubilities are very similar.

The apparent atomic radii for the rare earths are significantly smaller than the pure metal radii indicating negative deviations from Vegard's law. Friedel (5) has expressed the deviations from Vegard's law as:

$$y = C_B(d_B - d_A)(X_A/X_B - 1) / \left\{ [(1 + \sigma_A)X_A / 2(1 + \sigma_A)X_B] + 1 \right\}$$

where,

- y = deviation
- C_B = decimal equivalent of the atomic concentration of solute
- d_B = radius of the solute
- d_A = radius of the solvent
- X_B = compressibility of solute
- X_A = compressibility of solvent
- σ_A = Poisson's ratio for solvent

Since the rare earth apparent atomic radii are larger than the gold radius and since the rare earth compressibilities

are larger than that of gold (see Table 7) negative deviations would be expected according to Friedel's theory. The necessary quantities for applying Friedel's expression to the rare earth-gold systems are given in Table 7.

Table 7. Data for calculating deviations from Vegard's law^a

Element	d	$\chi (\times 10^{-7} \text{ cm}^2/\text{kg})$	
Au	1.442	5.66	0.425
Sc	1.641	22.6	-
Lu	1.734	23.85	-
Tm	1.746	24.71	-
Er	1.757	23.88	-
Ho	1.766	24.72	-
Dy	1.773	25.5	-
Tb	1.782	24.5	-
Gd	1.802	25.6	-

^aValues taken from Gschneidner (23).

The values for the deviations from Vegard's law using Friedel's relationship are compared with those observed in the experimental data in Table 8. The agreement is very good for all cases except for Sc-Au. This strongly suggests that the rare-earth atoms are compressed by the environment of the gold lattice, and that these rare earths which show significant solubility are compressed to a size within the favorable size factor range of gold. Perhaps the large electronegativity difference or the fact that the compressed atoms are on the borderline of favorable size factor are the reasons that the solubilities are less than 10 atomic percent in all cases.

Table 8. Deviations from Vegard's law

System	Experi- mentally obsv. dev.	Deviation from Friedel	Composition at which dev. calc.
Sc-Au	-0.0090	-0.0042	6.2 a/o Sc
Lu-Au	-0.0065	-0.0066	6.3 a/o Lu
Tm-Au	-0.0066	-0.0066	5.9 a/o Tm
Er-Au	-0.0059	-0.0058	5.2 a/o Er
Ho-Au ^a	-	-0.0048	4.0 a/o Ho
Dy-Au	-0.0026	-0.0026	2.1 a/o Dy
Tb-Au	-0.0018	-0.0019	1.5 a/o Tb
Gd-Au	-0.0009	-0.0008	0.6 a/o Gd

^aValue calculated using Wunderlin et al. (2) data.

It is interesting to note the changes occurring for the rare earths using their apparent atomic radii and Gordy's method (18) to calculate their electronegativities. The results of this are compared with the electronegativities calculated from their pure metal radii in Table 9.

Table 9. Electronegativities

Element	Electroneg. χ (a.s.r.)	Electroneg. χ (pure metal radius)
Sc	1.29	1.27
Lu	1.26	1.22
Tm	1.25	1.22
Er	1.25	1.22
Dy	1.23	1.21
Tb	1.22	1.21
Gd	1.20	1.20

There is a larger change in the electronegativities of the more soluble rare earths than there is in the less soluble ones. The change is in the right direction (toward the value for gold) but it is not large enough to bring the rare earth electronegativities within 0.4 units of the value for gold.

An effort was made to determine the solubilities of the light rare earths which were lanthanum, cerium, neodymium, samarium, and yttrium. The slopes of the lattice parameter versus composition curves in the single phase region, i.e. the change in lattice constant / change in composition, for the heavy rare earths and scandium were plotted against their radii (see Figure 8). It is seen that there are two possible branches (A and B) to the curve. The A branch assumes the values for terbium and gadolinium are valid and the B branch assumes an error in these values. Then the extrapolated slopes for five rare earth systems were taken from the curves and used to determine the solid solubility limits. It was assumed that the alloys of the light rare earths were in two phase regions. Then from the slopes and the lattice parameters of these alloys the solubilities were calculated using the relationship:

$$a/\text{slope} = c$$

where

a = lattice constant of solid solution

c = solubility limit

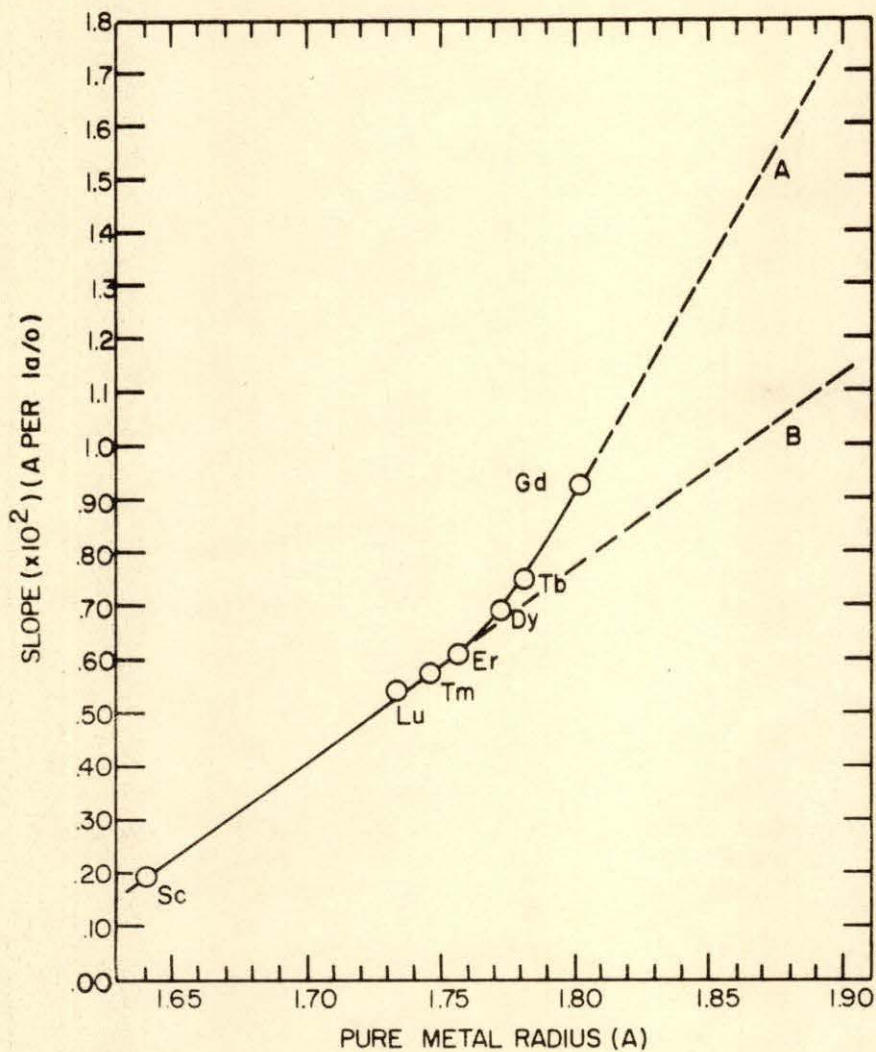


Figure 8. The slope of the lattice constant versus composition line plotted against pure metal radii of some of the rare earth metals.

The solubilities obtained in using either branch resulted in only slightly different values. In Figure 9, the solubilities determined in the above indirect manner plus those obtained directly from the experimental data are plotted versus atomic number. One notes a gradual increase from lanthanum to gadolinium and a sharp increase beginning at gadolinium. Although the light rare earths have larger compressibilities than the heavy rare earths, they apparently cannot be compressed such that their sizes are within the favorable range for solubility in gold. Thus, they have only slight solubilities in gold. The solubilities for terbium and dysprosium are intermediate and may be due to the fact that their size factors are just slightly greater than 15 percent.

The case of scandium is interesting because of its large deviation from Vegard's law, compared to the calculated value, and its rather low solubility in relation to its adjusted size factor (4.5 percent). Yttrium is also interesting because it has a pure metal radius almost identical to gadolinium yet it is over three times as soluble. These observations appear somewhat contradictory because scandium would be predicted to be more soluble and yttrium less soluble. The compressibility difference between yttrium and gadolinium ($26.8 \times 10^{-7} \text{ cm}^2/\text{kg}$ for yttrium and $25.6 \times 10^{-7} \text{ cm}^2/\text{kg}$ for gadolinium) might be the reason for the divergent solubilities. It is possible that yttrium is compressed to a more favorable

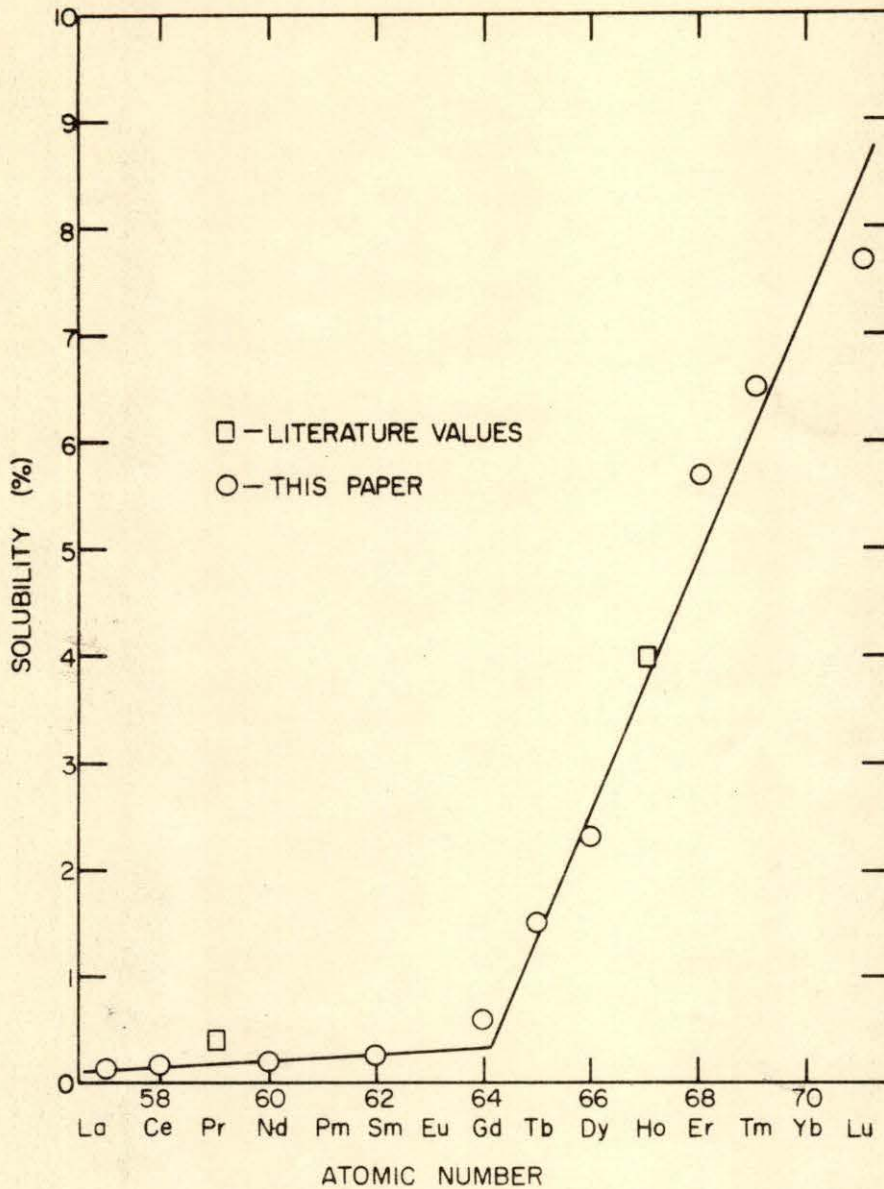


Figure 9. Solubility (a/o) of the rare earth metals in gold versus the atomic number. The value for the Pr-Au system was taken from Gschneidner (21).

size than gadolinium. By extrapolating the lattice constant versus composition line for yttrium to 100 percent solute, however, the apparent atomic radius becomes 1.74A which is still 21 percent larger than the radius of gold. The explanation for the scandium case might lie in the free energies of the first compounds on the gold-rich side of the phase diagrams for Sc-Au and Lu-Au. Possibly, scandium is less soluble than expected because the first compound has a higher gold content in the Sc-Au system than in the Lu-Au system. Consequently, the first scandium-gold compound might have a lower free energy than the first lutetium-gold compound with the result being that the two systems exhibit similar solubilities even though scandium has a much more favorable size factor.

Wunderlin, et al. (2) also found solubilities of 1.6 atomic percent holmium in silver and 0.02 atomic percent holmium in copper. By applying Friedel's (5) theory to these cases, the size factors become 15.6 percent for Ho-Ag and 22 percent for Ho-Cu. These values indicate that the solubilities observed are consistent with the 15 percent size factor.

In relating the solubilities in this investigation to strain energies in the solvent lattice, consideration was given to the square of the size factor which, according to Jaswon et al. (24), is proportional to the strain energy. Solubilities are plotted against the squares of the size factors in Figure 10 and it can be seen that there is an increase

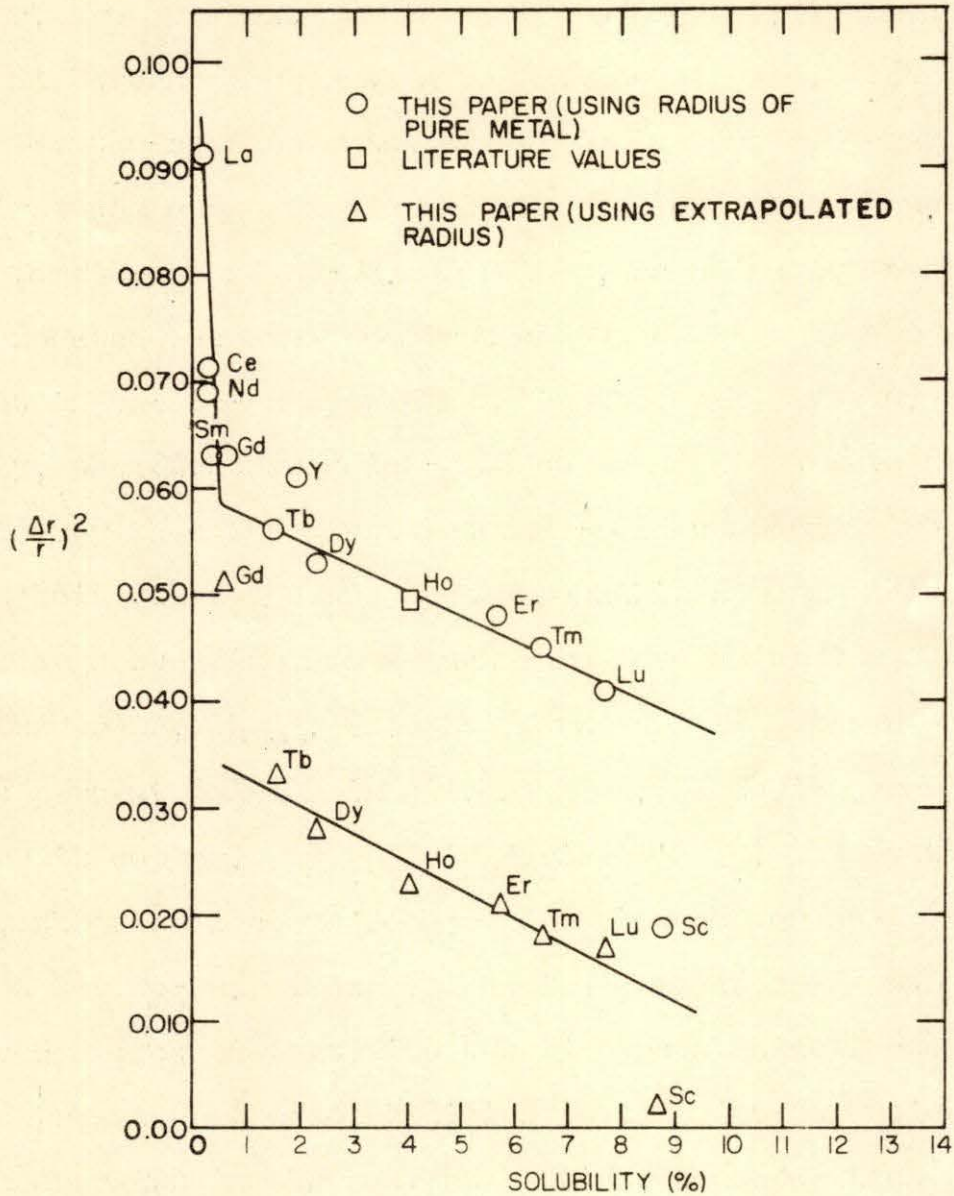


Figure 10. Square of the size difference (which is proportional to the strain energy) versus solubility (a/o) of the rare earth metals in gold. The value for Ho was calculated from the data of Wunderlin *et al.* (2).

in solubility as the strain energy decreases. The size factors for both pure metal radii and extrapolated (apparent atomic) radii were used. Both curves show the same form but as is evident, the strain energies for the extrapolated radii are much less than those for the pure metal radii. Scandium in gold has quite a low strain energy again indicating that some other factor than size plays an important role in its solubility behavior. Yttrium in gold has a strain energy somewhat higher than would be expected for its solubility which again suggests some other factor also contributes in this case.

B. Eutectic Temperatures

The interesting behavior of the eutectic temperatures in the rare-earth in gold systems is plotted in Figure 11 as eutectic temperature versus atomic number. At erbium the eutectic temperature begins to rise. This is also the point at which the size factor becomes favorable for solid solution formation. Apparently this is an indication of a connection between the size factor becoming more favorable and eutectic temperature. A second plot of eutectic temperatures versus atomic radii is given in Figure 12 to include scandium.

According to Hume-Rothery (1), the shape of the liquidus curve versus composition in a binary metal system is greatly influenced by the size factor. As the size factor becomes less favorable, the liquidus curve develops a minimum in its

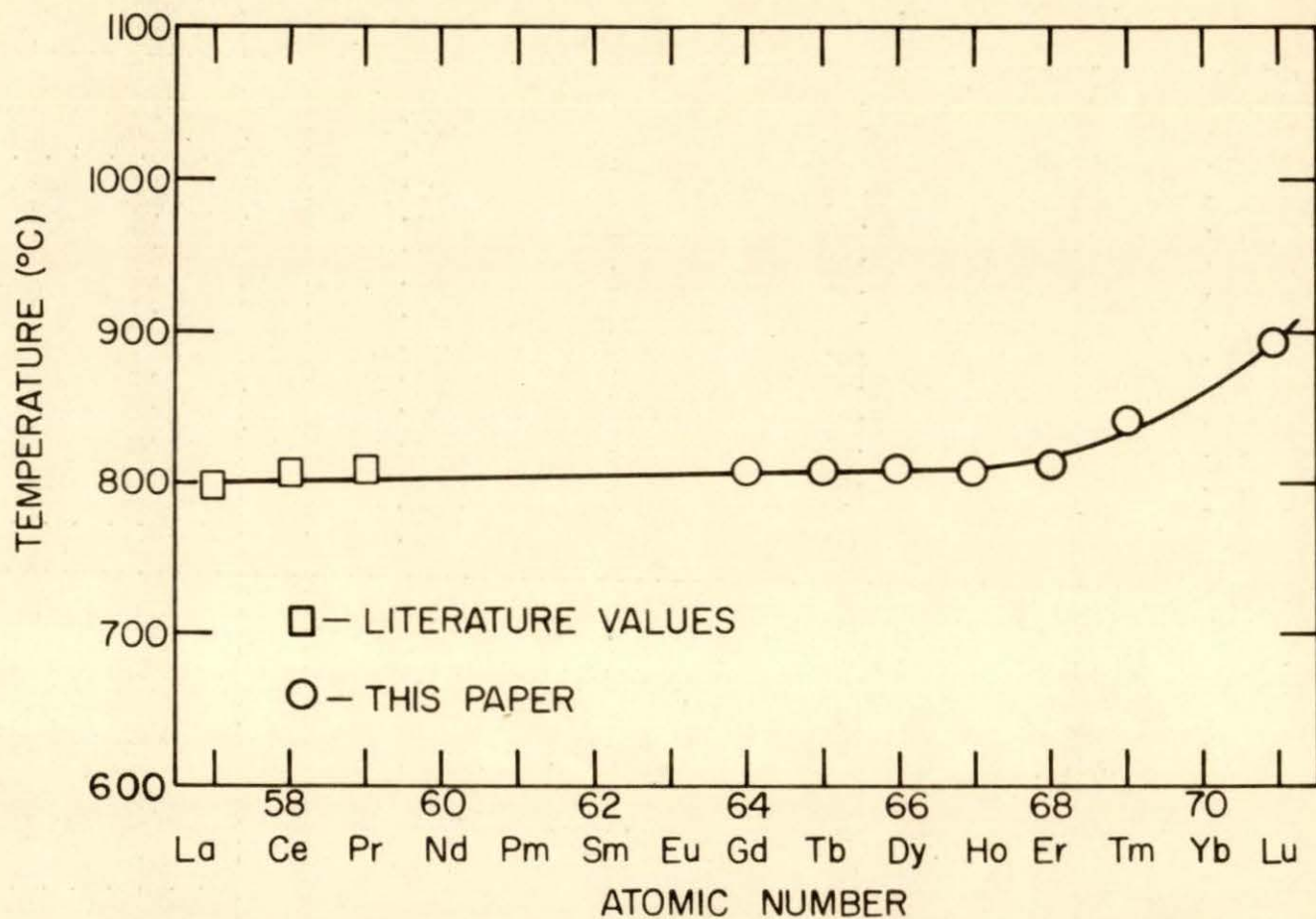


Figure 11. Eutectic temperatures of the rare earth-gold systems versus atomic numbers of the rare earth metals. The values for La, Ce, and Pr were taken from Gschneidner (21).

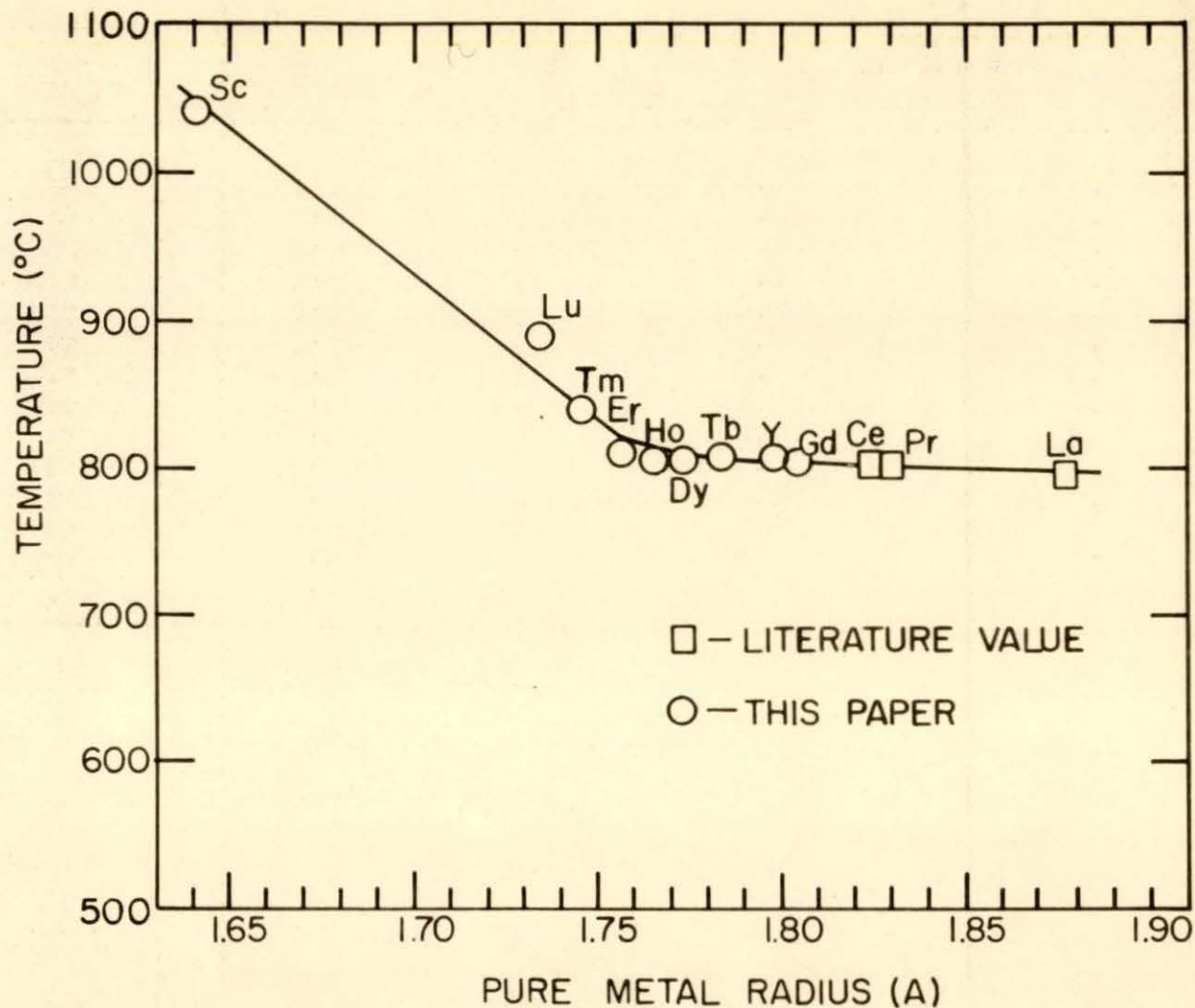


Figure 12. Eutectic temperatures of the rare earth-gold systems versus pure metal radii of the rare earth metals. The values for La, Ce, and Pr were taken from Gschneidner (21).

(the eutectic temperature corresponds to this minimum). As the size factor becomes more favorable this minimum begins to rise and the liquidus curve tends to flatten out. From Figure 12 it can be seen that scandium has a eutectic temperature far above that of lutetium and the other rare earths. The adjusted size factors in Table 6 show that scandium has a much more favorable size factor than the other rare earths (4.5 percent compared to 13.0 percent for lutetium) adding evidence to the effect of size factor on eutectic temperature. Generally speaking, the effect of size factor on eutectic temperatures is further substantiated by the fact that the eutectic temperatures begin to rise just as the size factor becomes favorable at erbium.

VI. CONCLUSION

The results of this study show that in some cases of predicting solubility behavior, the complex nature of the substances involved must be considered quite carefully. Very little solubility would be expected for the rare-earth metals in gold by considering the Hume-Rothery criteria (1). But as was seen from these results, this is not the case. Application of the Friedel model (5) to these systems indicated that the relative size of the rare-earth atom changed substantially when placed in a gold lattice. This change would be expected to lead to negative deviations from Vegard's law if considered from the pure metal sizes. Deviations calculated from Friedel's model are within experimental error of being equal to the observed deviations. This mutual size adjustment appears to explain the abnormal solubilities found for the heavy rare earths because their apparent sizes in gold are within the favorable size range for solid solution formation in gold. Yttrium and scandium, which are not true rare earths, behave anomalously in relation to the other rare earths but unfortunately there is not enough experimental information to explain their behavior.

The eutectic temperatures found reflect the effect of the size factor on the liquidus line. As the size factor became more favorable for solid solution formation at erbium, the eutectic temperatures began to rise. This behavior would be

expected. The large increase in the eutectic temperature from lutetium to scandium can be correlated with the sharp decrease in size factor.

In summary, the solubility found by Wunderlin et al. (2) for holmium in gold, which instigated this study, appears to be valid, although some of their data is questionable. There is a definite trend in solubility of the rare earths in gold. Apparently the solubilities found can be readily explained on the basis of size considerations alone and no interpretation of the complex electronic distribution of the rare earths and its effect on solubility is necessary. The electronic characteristics apparently play a secondary role in the solubility behavior found here except for possibly scandium and yttrium.

VII. LITERATURE CITED

1. Hume-Rothery, W. and Raynor, G. V. The structure of metals and alloys. 3rd ed. Institute of Metals Monograph and Report Series 1. 1954.
2. Wunderlin, W., Beaudry, B. J., and Daane, A. H. The solid solubility of holmium in copper, silver, and gold. Trans. Met. Soc. of Am. Inst. Min. Met. and Pet. Engrs. 227: 1302. 1963.
3. Vegard, L. Die Konstitution der Mischkristalle und die Raumbullung der Atome. Z. Physik 5: 17. 1921. Original available but not translated; cited in Hume-Rothery, W. and Raynor, G. V. The structure of metals and alloys. 3rd ed. Institute of Metals Monograph and Report Series 1: 99. 1954.
4. Eshelby, J. D. The continuum theory of lattice defects. Solid State Physics 3: 79. 1951.
5. Friedel, J. Deviations from Vegard's law. Phil. Mag. 46: 514. 1955.
6. Gschneidner, K. A., Jr. and Vineyard, G. H. Departures from Vegard's law. J. Appl. Physics 33: 3444. 1962.
7. Averbach, B. E. The structure of solid solutions. Nat. Met. Congress and Exposition Proc. 37: 301. 1955.
8. Warren, B. E., Averbach, B. L., and Roberts, B. W. Atomic size effect in the x-ray scattering by alloys. J. Appl. Physics 22: 1493. 1951.
9. Goldschmidt, B. M. Uber Atomabstande in Metallen. Z. Physik Chem. 133: 397. 1928. Original available but not translated; cited in Darken, L. S. and Gurry, R. W. Physical chemistry of metals. p. 49. New York, N. Y. McGraw-Hill Book Co., Inc. 1953.
10. Axon, H. J. and Hume-Rothery, W. The lattice spacings of solid solutions of different elements in aluminum. Proc. Roy. Soc. 193A: 1. 1948.
11. Chessin, Henry, Arajs, Sigurds, and Miller, D. S. Lattice spacings in some transition metal terminal solid solutions. Appl. X-ray Anal. Proc. 11: 121. 1963.

12. Kleppa, O. J. Aspects of the thermodynamics of metallic solid solutions. *Metallic solid solutions*, pp. XXXIII-1 - XXXIII-25. New York, N. Y. W. A. Benjamin, Inc. 1963.
13. Slater, J. and Koster, G. Wave functions of impurity levels. *Phys. Rev.* 95: 1167. 1954.
14. Friedel, J. The distribution of electrons round impurities in monovalent metals. *Phil. Mag.* 43: 153. 1952.
15. Jones, H. Application of the Bloch Theory to the study of alloys. *Proc. Roy. Soc.* 147A: 396. 1934.
16. Darken, L. S. and Gurry, R. W. *Physical chemistry of metals*. New York, N. Y. McGraw-Hill Book Co., Inc. 1953.
17. Pauling, L. The nature of the chemical bond. IV. The energy of single bonds and the relative electronegativities of atoms. *J. Am. Chem. Soc.* 54: 3570. 1932.
18. Gordy, W. and Thomas, W. J. Electronegativities of the elements. *J. Chem. Physics* 24: 2. 1956.
19. Cullity, B. D. *Elements of x-ray diffraction*. Reading, Mass. Addison-Wesley Publ. Co., Inc. c1956.
20. Hansen, Max. *Constitution of binary alloys*. 2nd ed. New York, N. Y. McGraw-Hill Book Co., Inc. 1958.
21. Gschneidner, K. A., Jr. *Rare-earth alloys*. Princeton, N. J. D. Van Nostrand Co., Inc. 1961.
22. Weber, James T., Gschneidner, K. A., Jr., Larson, Allen, and Prince, M. Y. Prediction of solid solubility in metallic alloys. *Trans. Met. Soc. of Am. Inst. Min. Met. and Pet. Engrs.* 227: 717. 1963.
23. Gschneidner, K. A., Jr. Physical properties and interrelationships of the metallic and semimetallic elements. [To be published in *Solid State Physics*, 16. ca. 1964].
24. Jaswon, M. A., Henry, V. G., and Raynor, G. V. The cohesion of alloys I. Intermetallic systems formed by copper, silver, and gold, and deviations from Vegard's law. *Proc. Roy. Soc.* 64B: 177. 1951.

VIII. ACKNOWLEDGMENTS

The author wishes to express his appreciation to Dr. Karl Gechnidner for his assistance and very helpful advice during this investigation. Also, he would like to thank Paul Palmer and Bernie Beaudry for providing the rare earth metals and helping in the technical aspects of this study. A note of thanks goes to Robert Joseph for the many favors and helpful advice which he offered and a special note of thanks to my wife who helped me in so many ways.

IX. APPENDIX

Table 10. Data for pure gold and for light rare earths, yttrium, and lanthanum in gold systems

Composition (a/o)	Quenching temp. (°C.)	Lattice constant (Å)
Pure gold	780	4.0766 ₋₂
4.2 La	765	4.0785 ₊₁
4.2 La	798	4.0780 ₊₂
5.9 Ce	765	4.0783 ₊₂
5.2 Nd	765	4.0782 ₊₁
4.0 Sm	765	4.0792 ₊₁
3.0 Y	809	4.0938 ₊₂

Table 11. Data for the heavy rare earth in gold systems

Composition (a/o)	Quenching temp. (°C.)	Lattice constant (Å)
0.3 Gd-Au	780	4.0799 ₊₁
0.5 Gd-Au	780	4.0812 ₊₂
1.0 Gd-Au	780	4.0820 ₊₂
1.5 Gd-Au	780	4.0822 ₊₁
2.0 Gd-Au	950	4.0809 ₊₂
2.0 Gd-Au	850	4.0815 ₊₂
2.0 Gd-Au	780	4.0820 ₊₃
3.0 Gd-Au	850	4.0818 ₊₅
3.0 Gd-Au	780	4.0822 ₊₁
3.0 Gd-Au	740	4.0804 ₊₁₀
3.0 Gd-Au	700	4.0806 ₊₁
3.0 Gd-Au	600	4.0796 ₊₁
3.0 Gd-Au	500	4.0789 ₊₁
3.0 Gd-Au	400	4.0792 ₊₃
3.0 Gd-Au	300	4.0783 ₊₃
4.0 Gd-Au	780	4.0816 ₊₁
4.0 Gd-Au	740	4.0794 ₊₁
4.0 Gd-Au	700	4.0810 ₊₄
4.0 Gd-Au	600	4.0782 ₊₂
4.0 Gd-Au	500	4.0789 ₊₁
4.0 Gd-Au	400	4.0786 ₊₄
4.0 Gd-Au	300	4.0786 ₊₁

Table 11. (Continued)

Composition (a/o)	Quenching temp. (°C.)	Lattice constant (Å)
0.5 Tb-Au	809	4.0806+1
1.0 Tb-Au	809	4.0848+10
2.0 Tb-Au	850	4.0860+1
2.0 Tb-Au	809	4.0878+1
2.0 Tb-Au	700	4.0828+1
2.0 Tb-Au	500	4.0797+1
2.0 Tb-Au	300	4.0798+1
3.0 Tb-Au	950	4.0810+10
3.0 Tb-Au	850	4.0860+2
3.0 Tb-Au	809	4.0881+2
3.0 Tb-Au	700	4.0823+1
3.0 Tb-Au	500	4.0794+1
3.0 Tb-Au	300	4.0793+3
(samples annealed in air)		
0.5 Tb-Au	780	4.0773+3
1.0 Tb-Au	780	4.0781+3
2.0 Tb-Au	780	4.0789+4
3.0 Tb-Au	780	4.0782+2
0.5 Dy-Au	780	4.0811+2
1.0 Dy-Au	780	4.0836+2
2.0 Dy-Au	850	4.0902+2
2.0 Dy-Au	780	4.0920+1
3.0 Dy-Au	950	4.0821+2
3.0 Dy-Au	850	4.0903+2
3.0 Dy-Au	780	4.0930+2
4.0 Dy-Au	950	4.0852+5
4.0 Dy-Au	780	4.0924+3
4.0 Dy-Au	740	4.0891+2
4.0 Dy-Au	700	4.0882+4
4.0 Dy-Au	600	4.0835+4
4.0 Dy-Au	500	4.0808+1
4.0 Dy-Au	400	4.0791+1
4.0 Dy-Au	300	4.0794+2
5.0 Dy-Au	780	4.0928+1
5.0 Dy-Au	740	4.0885+2
5.0 Dy-Au	700	4.0868+2
5.0 Dy-Au	600	4.0825+2
5.0 Dy-Au	500	4.0813+2
5.0 Dy-Au	400	4.0796+2
5.0 Dy-Au	300	4.0808+7

Table 11. (Continued)

Composition (a/o)	Quenching temp. (°C.)	Lattice constant (Å)
0.6 Er-Au	780	4.0816±1
1.2 Er-Au	780	4.0832±1
2.3 Er-Au	780	4.0936±10
3.5 Er-Au	780	4.0958±2
4.7 Er-Au	850	4.1027±3
4.7 Er-Au	780	4.1054±3
6.0 Er-Au	950	4.0949±3
6.0 Er-Au	850	4.1054±4
6.0 Er-Au	780	4.1085±2
6.0 Er-Au	740	4.1089±2
6.0 Er-Au	700	4.1050±4
6.0 Er-Au	600	4.0930±3
6.0 Er-Au	500	4.0843±10
6.0 Er-Au	400	4.0808±2
6.0 Er-Au	300	4.0830±4
8.0 Er-Au	780	4.1078±5
8.0 Er-Au	740	4.1087±3
8.0 Er-Au	700	4.1040±4
8.0 Er-Au	600	4.0934±2
8.0 Er-Au	500	4.0873±11
8.0 Er-Au	400	4.0814±3
8.0 Er-Au	300	4.0808±2
2.0 Tm-Au	1000	4.0884±2
2.0 Tm-Au	780	4.0878±2
4.0 Tm-Au	780	4.0999±2
6.0 Tm-Au	890	4.1032±2
6.0 Tm-Au	850	4.1112±2
6.0 Tm-Au	780	4.1107±3
6.0 Tm-Au	740	4.1086±2
6.0 Tm-Au	700	4.1057±3
6.0 Tm-Au	600	4.0950±2
6.0 Tm-Au	500	4.0879±9
6.0 Tm-Au	400	4.0822±1
6.0 Tm-Au	300	4.0816±2
8.0 Tm-Au	780	4.1103±3
8.0 Tm-Au	600	4.0986±25
8.0 Tm-Au	500	4.0876±1
8.0 Tm-Au	400	4.0821±2
8.0 Tm-Au	300	4.0815±3

Table 11. (Continued)

Composition (a/o)	Quenching temp. (°C.)	Lattice constant (Å)
0.5 Lu-Au	780	4.0812±2
1.0 Lu-Au	780	4.0835±2
2.0 Lu-Au	780	4.0873±2
4.0 Lu-Au	780	4.0981±2
6.0 Lu-Au	780	4.1096±2
8.0 Lu-Au	890	4.1169±1
8.0 Lu-Au	850	4.1153±2
8.0 Lu-Au	780	4.1105±2
8.0 Lu-Au	740	4.1078±1
8.0 Lu-Au	600	4.0950±3
8.0 Lu-Au	500	4.0891±4
8.0 Lu-Au	400	4.0834±4
8.0 Lu-Au	300	4.0830±5
9.0 Lu-Au	890	4.1183±3
9.0 Lu-Au	740	4.1072±2
9.0 Lu-Au	600	4.0965±11
9.0 Lu-Au	500	4.0890±2
9.0 Lu-Au	400	4.0824±2
9.0 Lu-Au	300	4.0830±3
3.0 Sc-Au	780	4.0822±1
6.0 Sc-Au	780	4.0872±2
9.0 Sc-Au	1000	4.0912±1
9.0 Sc-Au	950	4.0908±2
9.0 Sc-Au	850	4.0898±2
9.0 Sc-Au	780	4.0878±2
9.0 Sc-Au	740	4.0872±2
9.0 Sc-Au	700	4.0876±6
9.0 Sc-Au	500	4.0810±2
9.0 Sc-Au	400	4.0802±3
9.0 Sc-Au	300	4.0800±3
12.0 Sc-Au	1000	4.0917±2
12.0 Sc-Au	780	4.0881±2
12.0 Sc-Au	700	4.0866±3
12.0 Sc-Au	600	4.0845±2
12.0 Sc-Au	500	4.0814±5
12.0 Sc-Au	400	4.0802±5
12.0 Sc-Au	300	4.0800±4